Zeolite-Induced Solvation Effects on Excited-State Properties of $Ru(bpy)_3^{2+}$: Implications for Intrazeolitic Photochemical Quenching Reactions†

Michael A. Coutant, Ty Le, Norma Castagnola, and Prabir K. Dutta*

Department of Chemistry, The Ohio State University, 100 West 18th Avenue, Columbus, Ohio 43210

Received: February 14, 2000; In Final Form: May 11, 2000

Photosensitized electron-transfer reactions between tris(2,2′-bipyridine)ruthenium(II) ($Ru(bpy)_3^{2+}$) and bipyridinium ions have been extensively studied. Entrapment of this donor−acceptor system in zeolite Y retards the back electron transfer as compared to the forward electron transfer and appears to be an effective system for the photogeneration of long-lived charge-separated species. In this paper, we evaluate how the properties of the photoexcited zeolite-entrapped $Ru(bpy)_3^{2+}$ change as it is surrounded by bipyridinium ions. However, most bipyridinium ions quench the excited state of $Ru(bpy)_3^{2+}$ and the characteristic properties of the excited state of $Ru(bpy)_3^{2+}$ cannot be monitored. So, we have used tetraethylammonium (TEA) to surround the zeolite-entrapped $Ru(bpy)_3^{2+}$, which helps mimic the effect of the presence of large organic cations, while avoiding the problem of quenching. Upon exchange of TEA, a blue shift in the fluorescence emission of 21 nm, an increase in the emission intensity by a factor of 2.7, and an increase in the lifetime of excited $Ru(bpy)_3^{2+}$ by a factor of 2 are observed. We propose that these effects are a result of the intrazeolitic bulk-like uncomplexed water being displaced by the TEA ions. The remaining water molecules are held tightly by the framework and the sodium cations, creating an environment typical of a frozen medium. Similar effects should occur when the intrazeolitic $Ru(bpy)_3^{2+}$ is surrounded by bipyridinium ions. Indeed, very unexpected quenching data and emission spectra are observed for $Ru(bpy)_3^{2+}$ in zeolite Y in the presence of the quencher *N*,*N*′-dimethyl-2,2′-bipyridinium ion. This quencher has a large reduction potential (−0.72 V), thereby inefficiently quenching $Ru(bpy)_3^{2+}$* and making it possible to observe the emission spectrum. The implications of this study are that in the $Ru(bpy)_3^{2+}$−bipyridinium system in zeolite Y, the photoexcited reactant $Ru(bpy)_3^{2+}$* has a longer lifetime and should promote the extent of the forward electron-transfer reaction to the bipyridinium ions in neighboring cages.

Introduction

Utilization of the ordered topology of zeolites to provide molecular level organization of photochemical systems is an active area of research.[1,2] A system that has been extensively studied is tris(2,2′-bipyridine)ruthenium(II) encapsulated within the supercages of zeolite Y ($Ru(bpy)_3^{2+}$−Y).[3−6] The radius of $Ru(bpy)_3^{2+}$ is ∼12 Å[7] and ensures a tight fit within the ∼13 Å supercage, yet allowing for effective interaction with molecules in neighboring cages via the four 7 Å windows. Of particular interest to us and other research groups has been the study of the mechanism of the electron transfer from photoexcited $Ru(bpy)_3^{2+}$−Y to acceptor molecules in neighboring cages.[8−12] The eventual goal of these studies is to promote long-lived charge separation by exploiting features of the zeolite. Recently, we have shown that as compared to the forward electron transfer from $Ru(bpy)_3^{2+}$* to bipyridinium ions within the zeolite, the back electron transfer is considerably slower, resulting in long-lived charge-separated states.[12]

Zeolites not only provide for novel spatial arrangements of molecules but also provide ways to introduce steric constraints and a novel solvation environment. Properties of $Ru(bpy)_3^{2+}$ are known to be strongly medium dependent.[13−17] In this study, we focus on how the photophysics of $Ru(bpy)_3^{2+}$ in zeolite Y is altered as large organic cations are ion-exchanged into the zeolite. A major physical effect of these ions is to displace the water molecules and has been referred to in the zeolite literature as the "water-transfer effect", which should result in an altered intrazeolitic environment.[18] The reason we embarked on this study is that in the $Ru(bpy)_3^{2+}$−bipyridinium system, the bipyridinium ions exchanged into the zeolite must also be replacing the intrazeolitic water. Our goal was to evaluate how this altered environment influences the photoexcited properties of $Ru(bpy)_3^{2+}$ and hence the forward electron transfer from $Ru(bpy)_3^{2+}$* to bipyridinium ions. We succeeded in mimicking the effect of bipyridinium ions by ion-exchanging with tetraethylammonium (TEA) cations, which should have no photochemical interaction with $Ru(bpy)_3^{2+}$, yet is reasonably large in size and resembles the occupancy by the bipyridinium ions.

The properties of the $Ru(bpy)_3^{2+}$−TEA−zeolite Y system were studied using fluorescence spectroscopy, temperature-dependent lifetime studies, diffuse reflectance, and Raman spectroscopy. A modified Franck−Condon analysis was performed in order to extract parameters about the excited state of $Ru(bpy)_3^{2+}$. From temperature-dependent lifetime data of $Ru(bpy)_3^{2+}$, information about rate constants of the decay from the excited state was obtained. We find that the presence of TEA increases the emission quantum yield and lifetime of $Ru(bpy)_3^{2+}$* and the emission maximum is blue-shifted. By using a bipyridinium molecule that only weakly quenches $Ru(bpy)_3^{2+}$*, it has been confirmed that the presence of bipyridinium ions neighboring to $Ru(bpy)_3^{2+}$ leads to enhancement of emission intensity and shifts of emission maximum to higher energies. The implication here is that in the zeolite, $Ru(bpy)_3^{2+}$* in the presence of bipyridinium ions should have

† Part of the special issue "Thomas Spiro Festschrift".

10.1021/jp000601c CCC: $19.00
Published on Web 06/27/2000

longer excited-state lifetimes, thus facilitating the extent of the forward electron transfer.

Experimental Section

The synthesis and purification of zeolite-entrapped $Ru(bpy)_3^{2+}$ has been described in previous work.[3−5] Zeolite Y (Union Carbide) was calcined and washed extensively with 1 M NaCl. This zeolite was then exchanged with $Ru(NH_3)_6^{3+}$ at a loading of 1 molecule of $Ru(NH_3)_6^{3+}$ in 30 supercages. These samples were air-dried and mixed with a 0.006 M bipyridine solution in ethanol. After extensive mixing, the ethanol was evaporated under nitrogen and the remaining powder was heated (200 °C) under vacuum for 24 h. The synthesis yielded a yellow-orange powder of zeolite-entrapped $Ru(bpy)_3^{2+}$. This was followed by Soxhlet extraction with ethanol to remove excess bipyridine, followed by washing in 1 M NaCl. For TEA exchange, 200 mg pellets were treated with solutions of 1 M TEABr several times.

UV−vis diffuse reflectance spectra were obtained using a Shimadzu UV-265 spectrometer with a HVC-DRP reflective attachment, built by Harrick Scientific. Emission spectra were measured using a Spex Fluorolog fluorometer at an excitation wavelength of 450 nm. Spectra were collected using the DM3000F (version 3.3) software. The emission spectra were corrected for the lamp emission profile. Fluorescence lifetimes were measured using 532 nm radiation from a Quantel YG581 Nd:YAG laser (15 ns pulse widths) pulsed at 1 Hz. The photomultlipier signal at 620 nm was sent to a Tektronix DSA 601 Digitizing analyzer oscilloscope, where 256 decays were collected and averaged. The decays were exported and analyzed using SigmaPlot (Jandel Scientific). The temperature dependence of the lifetimes was measured with the help of an Oxford DN1704 liquid nitrogen cryostat with ITC 502 intelligent temperature controller. Temperatures were varied in a random manner with at least 10 min between temperature changes to ensure sample equilibration. A variation of ±0.1 K was achieved. Resonance Raman spectra were collected using a Coherent 90C-6 Ar^+ laser (457.9 nm) as the excitation source and a liquid nitrogen cooled charge-coupled detector (Princeton Instruments LNCCD-1100 PB UV-AR). Data were collected using CSMA data analysis program and transferred to Grams 32 (Galactic Industries). Acetaminophen was used as a reference to define the spectral shift.

Carbon and nitrogen analysis on TEA−zeolite was performed by Galbraith Laboratories, Inc. using the American Society for Testing Materials D5373/D5291 method, with the results of the analysis being 6.93% C and 0.93% N.

Results

(a) Studies of $Ru(bpy)_3^{2+}$−TEA−Y. As-synthesized $Ru(bpy)_3^{2+}$−Y was extensively ion-exchanged with 1 M TEABr solutions in order to obtain maximum exchange with the Na^+ cations. The TEA cation is too large to penetrate into the sodalite cage and can only be present in the supercages. To determine the loading levels of the TEA in the zeolite, the exact procedure of ion exchange as with $Ru(bpy)_3^{2+}$−Y was repeated with just Na−Y, followed by a C and N elemental analysis. On the basis of this analysis, the TEA loading was determined to be 1.45 molecules per supercage (assuming 470 μmol/g of zeolite). This loading of TEA should be similar in $Ru(bpy)_3^{2+}$−Y, since only 1 $Ru(bpy)_3^{2+}$ was present per 30 supercages.

Figure 1a compares the fluorescence emission of $Ru(bpy)_3^{2+}$−TEA−Y and $Ru(bpy)_3^{2+}$−Y. Two changes are noticeable. There is an increased intensity (2-fold) of the emission upon surrounding the $Ru(bpy)_3^{2+}$ by TEA ions in the neighboring supercages as well as a blue-shifting of the emission maximum from 626 to 605 nm. Absorption spectra and resonance Raman spectra showed no changes upon replacement of Na^+ by TEA. Figure 1b compares the lifetimes of zeolite−Y-entrapped $Ru(bpy)_3^{2+}$ exchanged with sodium and TEA ions. There is a lengthening of the lifetime in TEA−Y. To extract the lifetime of $Ru(bpy)_3^{2+}$, several models were examined, including single exponential, double exponential, and the Albery model. The Albery model assumes a Gaussian distribution of lifetimes around a single value.[19] Best fits to the data were obtained using the Albery model, and previous work has justified using this model because of the heterogeneous environment in the zeolite.[10] Two parameters were extracted from the fit, γ, which provides a measure of the spread of the Gaussian distribution and lifetime, τ, related to the mean rate constant of emission decay. Fits to the data in Na− and TEA−Y are also shown in Figure 1b. The calculated room-temperature lifetime τ (γ) of $Ru(bpy)_3^{2+}$−Y increases from 620 ns (0.69) in the sodium-exchanged sample to 1220 ns (0.61) in the TEA sample.

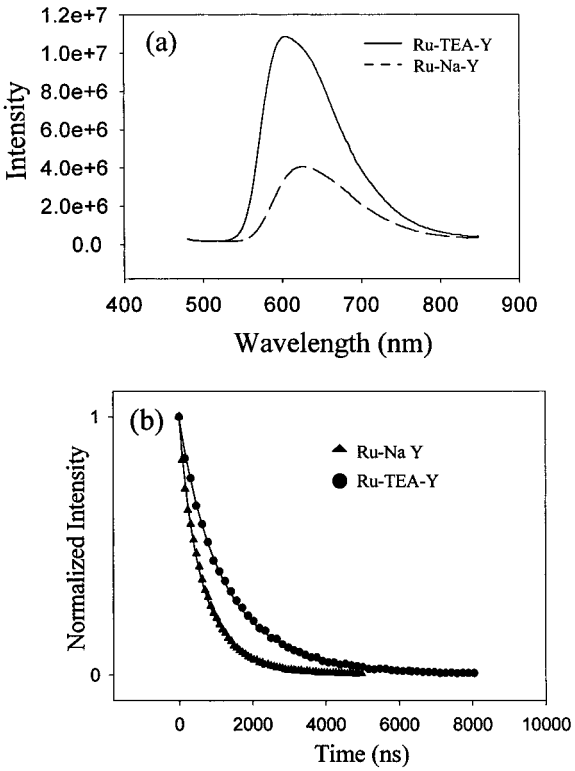

Figure 1. (a) Comparison of the emission spectra of $Ru(bpy)_3^{2+}$ in Na−Y and TEA−Y. (b) Comparison of the emission decay of $Ru(bpy)_3^{2+}$ at 610 nm in Na−Y and TEA−Y. Solid lines through the plots are fits to the data.

Temperature-dependent lifetimes were measured for $Ru(bpy)_3^{2+}$ in Na−Y and TEA−Y between 200 and 300 K, and the data are shown in Figure 2. These data were fit to eq 1,

$$\tau^{-1}(t) = k_1 + k_2 e^{-\Delta E/kT} \quad (1)$$

where $\tau(t)$ is the temperature-dependent lifetime, k_1 and k_2 are rate constants, and ΔE is an energy difference term. Use of eq 1 to describe the temperature dependence of lifetimes has been reported previously.[20] In this equation k_1 represents the sum of radiative (k_r) and nonradiative rate (k_{nr}) constants representing decay from an excited state. The temperature-dependent term indicates the existence of another excited-state ΔE above the first excited state with rate constants k_2 ($k_r + k_{nr}$). Best fits to

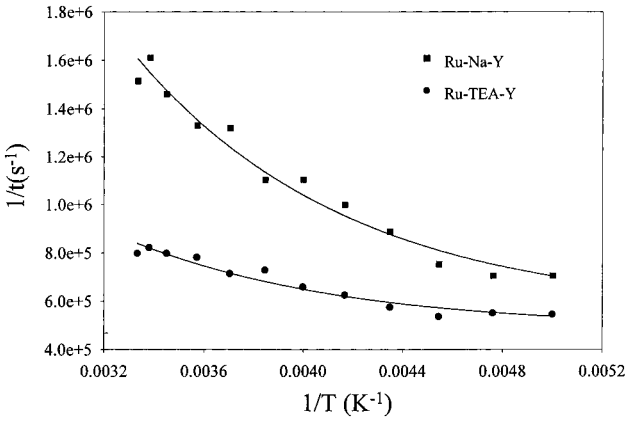

Figure 2. Dependence of the emission lifetimes of $Ru(bpy)_3^{2+}$ in Na−Y and TEA−Y on temperature. Solid lines are fit to the data using eq 1.

TABLE 1

compound	k_1, $s^{-1} \times 10^{-5}$	k_2, $s^{-1} \times 10^{-7}$	ΔE, cm^{-1}
$Ru(bpy)_3^{2+}$−Z[a]	3.8	11	890
$Ru(bpy)_3^{2+}$−CA[b]	10	1.7	810
$Ru(bpy)_3^{2+}$−Na−Y	5.5	4.9	800
$Ru(bpy)_3^{2+}$−TEA−Y	4.9	1.6	800

[a] Z = zeolite.[5] [b] CA = cellulose acetate.[13]

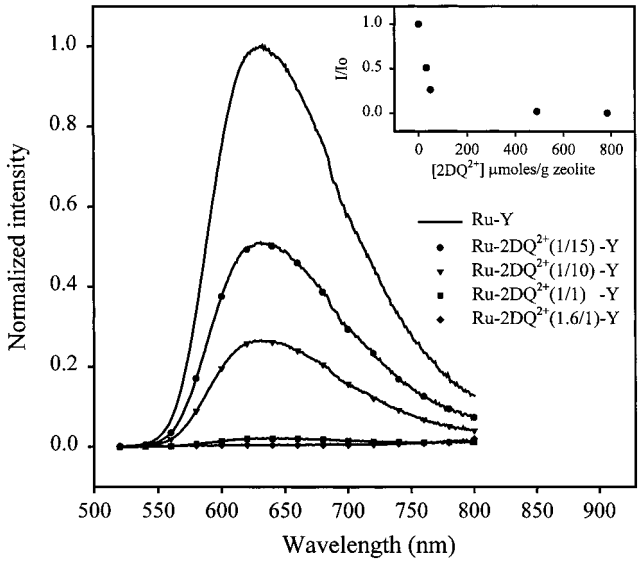

Figure 3. Quenching of the emission of $Ru(bpy)_3^{2+}$−Y with increased loadings of $2DQ^{2+}$ bipyridinium ions. The inset shows the emission intensity changes with intrazeolitic loading of $2DQ^{2+}$, loading levels are reported as molecule of bipyridinium ion per supercage e.g 1/15 refers to 1 $2DQ^{2+}$ per 15 supercages.

both the Na−Y and TEA−Y were obtained with a $\Delta E \approx 800$ cm^{-1} (solid line in Figure 2). Table 1 lists the rate constants obtained from eq 1 along with results from previous studies done in heterogeneous media, such as cellulose acetate[13] and Na− zeolite Y.[5]

(b) Studies of $Ru(bpy)_3^{2+}$−Bipyridinium−Zeolite. Two bipyridinium ions with different reduction potentials were examined as electron-transfer quenching reactants. These were ion-exchanged into $Ru(bpy)_3^{2+}$−Na−Y at various loading levels until saturation loading and the emission spectrum of $Ru(bpy)_3^{2+}$ was monitored. The bipyridinium ions were *N,N′*-dimethylene-2,2′-bipyridinium ($2DQ^{2+}$) and *N,N′*-dimethyl-2,2′- bipyridinium (N-$MeDQ^{2+}$). The reduction potentials of $2DQ^{2+}$ and N-$MeDQ^{2+}$ are −0.37 and −0.72 V (vs NHE), respectively.[21]

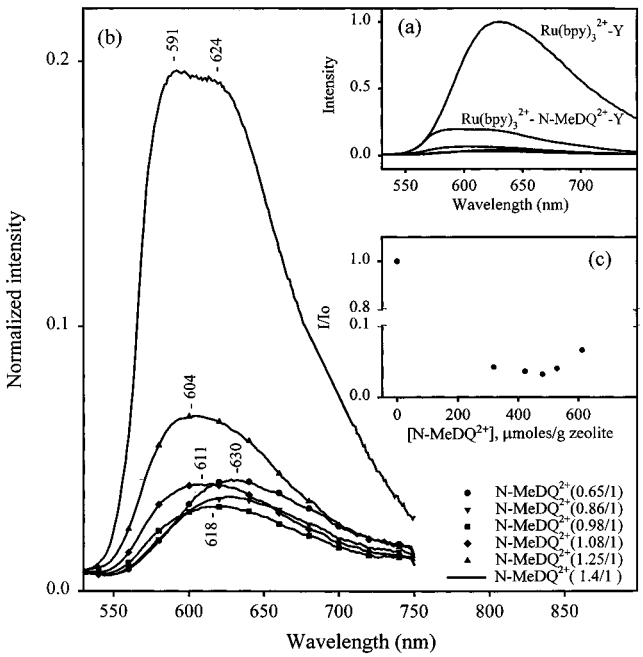

Figure 4. Quenching of the emission of $Ru(bpy)_3^{2+}$−Y by N-$MeDQ^{2+}$. (a) Emission spectra of $Ru(bpy)_3^{2+}$ and upon exchange with various loadings of N-$MeDQ^{2+}$ (loadings shown in lower left of the figure). (b) Expanded view of the emission spectra shown in Figure 4a, excluding the spectrum of $Ru(bpy)_3^{2+}$−Y. (c) Change in peak emission intensity as a function on N-$MeDQ^{2+}$ loading.

Figure 3 shows the change in emission spectra as a function of $2DQ^{2+}$ loading into the zeolite, along with a plot of the change in emission intensity with loading (inset). Similar data are shown in Figure 4 for N-$MeDQ^{2+}$. Figure 4a is the emission quenching as a function of N-$MeDQ^{2+}$ loading (varying from 0.65 to 1.4 N-$MeDQ^{2+}$ per supercage). These data have been expanded in Figure 4b without the spectrum of the parent $Ru(bpy)_3^{2+}$−Y to show the intensity changes clearly. Figure 4c is a plot of the maximum intensity as a function of N-$MeDQ^{2+}$ loading. The decrease in the emission intensity of $Ru(bpy)_3^{2+}$ arises from the electron-transfer quenching of $Ru(bpy)_3^{2+}$* by the bipyridinium ion. For $2DQ^{2+}$, the driving force for the electron-transfer reaction is +0.47 V as compared to +0.12 V for N-$MeDQ^{2+}$. In the case of $2DQ^{2+}$, the emission intensity essentially decreases to zero with increasing loadings. However, for N-$MeDQ^{2+}$, beyond a loading of about 1 bipyridinium ion per supercage, the emission intensity actually increases with loading of N-$MeDQ^{2+}$. The emission maximum also exhibits a progressive blue shift, with a peak at 591 nm at the highest loadings. No noticeable shifts in the bandwidths (fwhm ∼ 120−130 nm) were observed upon ion exchange.

Discussion

(a) Emission Spectra. Information about excited-state parameters of $Ru(bpy)_3^{2+}$ was obtained by fitting the emission bands using a modified Franck−Condon analysis that included an anharmonic Morse potential and previously used by Hartmann et al.[17] The following expression was used to model the spectra:

$$I(E) = \sum_{\nu=0}^{4}\left[\left(\frac{E_{00} - \hbar\omega_m(\nu - (\nu^2+\nu)\chi_e)}{E_{00}}\right)^4 \times \frac{S_m^\nu}{\nu!}\exp\left(-4\ln(2) \times \left(\frac{E - E_{00} + \hbar\omega_m(\nu - (\nu^2+\nu)\chi_e)}{\hbar\omega_{1/2}}\right)^2\right)\right] \quad (2)$$

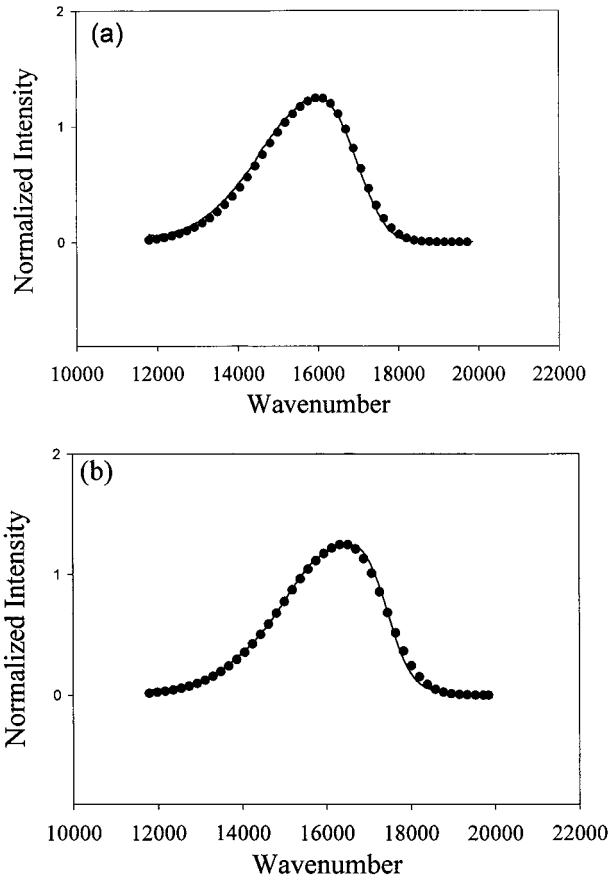

Figure 5. Fits of the emission spectra of (a) $Ru(bpy)_3^{2+}-Y$ and (b) $Ru(bpy)_3^{2+}-TEA-Y$. Solid lines are the experimental data and the calculated data are shown as dots.

TABLE 2: Fitting Parameters from Frank-Condon Analysis of Ru-X−Y

sample	E_{00} (cm^{-1})	S_m	$\hbar\omega_m$ (cm^{-1})	$\hbar\omega_{1/2}$ (cm^{-1})	χ_e
Ru−Na−Y	16296	0.94	1295	1680	0.01
Ru−TEA−Y	16790	0.98	1300	1720	0.01

In this equation, E_{00} is the energy difference between the zero point vibrational levels of the excited and ground states, S_m is the dimensionless fractional displacement of the effective normal mode between the equilibrium configurations of the ground and excited states, χ_e is the anharmonicity parameter of the Morse potential, $\hbar\omega_m$ is the effective energy of the relevant vibrations involved in excited-state relaxation, $\hbar\omega_{1/2}$ is the fwhm of an individual vibrational component, and ν are the vibrational sublevels that contribute to the emission profile. Figure 5 shows the fits of the emission spectra for $Ru(bpy)_3^{2+}$ in Na- and TEA-exchanged Y. The parameters extracted from these fits are listed in Table 2. The E_{00} for the $Ru(bpy)_3^{2+}-Y$ and $Ru(bpy)_3^{2+}-TEA-Y$ are calculated at 16 296 cm^{-1} (613.7 nm) and 16 790 cm^{-1} (595.6 nm), respectively. Values of $\hbar\omega_m$ of ~1300 cm^{-1} are consistent with the role of bipyridyl localized vibrations as the acceptor vibrations in the decay process.[17,22] The fractional displacement of the effective normal mode S_m (~1300 cm^{-1}) between the ground and excited states increases from 0.94 to 0.98 upon TEA exchange. An increase of S_m with an increase of E_{00} arises from an increased charge transfer in the excited state as the energy gap increases and is consistent with previous observations on Ru−polypyridyl complexes. [23]

(b) Lifetimes. The temperature dependence of the lifetimes of $Ru(bpy)_3^{2+}*$ in Na−Y and TEA−Y provide information about the rate constants and the energy levels of the states responsible for the temperature dependence of the decay.[20] The excited-state decay pathways of $Ru(bpy)_3^{2+}$ have been studied extensively. Upon excitation into the metal to ligand charge-transfer transition, a singlet excited state is formed that undergoes an effective ($\phi = 1$) intersystem crossing to the triplet ^{3}MLCT states.[24] These ^{3}MLCT states consist of a manifold of three closely spaced levels ($\Delta E = 60$ cm^{-1}), and in the temperature range of this study (200−300 K), these three lowest lying ^{3}MLCT states are in thermal equilibrium. The presence of the additional ^{3}MLCT state about 600−800 cm^{-1} above the manifold of the three low lying MLCT states has been observed in the single-crystal polarized emission spectra[25] and in solution.[26] There also lies a metal-centered ^{3}dd state about 3000 cm^{-1} above the lower ^{3}MLCT states.[20] In solution, the ^{3}dd state provides the efficient means of nonradiative decay resulting in either ligand loss or relaxation to the ground state. It has been previously reported that upon entrapment within solid matrices, such as cellulose acetate[13] and zeolite Y,[5] the ^{3}dd state becomes destabilized due to the steric constraints limiting the elongation of the Ru−N bond characteristic of this state. The increased energy of the state makes it thermally inaccessible and temperature dependence of the lifetimes was found to arise from thermal population of the fourth ^{3}MLCT state, 800−900 cm^{-1} above the manifold of the three MLCT states. In agreement with these previous studies, we find that in both TEA− and Na−Y, the temperature dependence of the lifetime arises from the fourth ^{3}MLCT state, which we calculate to be 800 cm^{-1} above the manifold of the three-MLCT states.

The two rate constants k_1 and k_2 that are obtained from the temperature−TEA lifetimes (Table 2) reflect the decay from the low lying manifold (set of three) MLCT state as well as the thermally activated fourth ^{3}MLCT state, respectively. Each rate constant has a radiative (k_r) and nonradiative (k_{nr}) component. It is known that for ^{3}MLCT states of $Ru(bpy)_3^{2+}$, $k_{nr} \gg k_r$ and the decay is dominated by the nonradiative component of the rate constant.[26] Previous studies have shown that the k_r component is relatively unaffected by environmental changes around $Ru(bpy)_3^{2+}$.[20] Thus, the change in k_1 and k_2 from 5.5×10^5 and 4.9×10^7 s^{-1} to 4.9×10^5 and 1.6×10^7 s^{-1} upon exchanging Na^+ by TEA is primarily arising from changes in k_{nr}. The fourth ^{3}MLCT state has more singlet character and should have a greater value of k_{nr},[27] consistent with the experimental data. We could not determine the contribution of k_r to k_1 and k_2, since quantum yields for these scattering samples could not be determined.

The increase in energy gap from 16 296 to 16 790 cm^{-1} upon replacing Na^+ with TEA should decrease the nonradiative decay and hence the lifetime of $Ru(bpy)_3^{2+}$ in TEA−zeolite Y should be higher than Na−zeolite Y, as is observed experimentally. On the basis of the formalism developed by Meyer and co-workers,[20a] it is possible to estimate the expected change in k_{nr} upon TEA exchange based on the change in the energy gap. This formalism takes into account only a single manifold of excited states as contributing to the decay. The parameters obtained by fitting the emission spectra (Figure 5, Table 2) E_{00}, S_m, ω_m were used to calculate k_{nr} and values of 2.24×10^5 and 1.6×10^5 s^{-1} for Na−Y and TEA−Y, respectively were obtained. The factor $C_k^2\omega_k$ which is a measure of the transition between the excited and ground states was taken to be 4.2×10^{17}, calculated from the data reported by Meyer and co-workers for $Ru(bpy)_3^{2+}$ in a series of non-hydroxylic solvents.[15] The decrease in k_{nr} predicted on the basis of the energy gap law in changing from Na−Y to TEA−Y is 29%, whereas the experimental data for k_1 and k_2 (both primarily k_{nr}) show a decrease

of 12% and 66% upon changing from Na−Y to TEA−Y. Not surprisingly, these calculations of k_{nr} demonstrate that it is important to take into account the fourth ^{3}MLCT state. For polypyridyl Os(II) complexes, it has also been noted that not considering the contributions of the fourth ^{3}MLCT state to k_{nr} resulted in poor correlation of theory and experiment.[22,26]

(c) Origin of the Spectral Perturbations Due to TEA Ions. The perturbations of $Ru(bpy)_3^{2+}$ in TEA−Y include a blue shift in the emission maximum and increases in both the quantum yield and lifetime of the excited state. The tetraethylammonium cation is not expected to have any electronic interaction with $Ru(bpy)_3^{2+}$. This is evident from the fact that no significant spectral perturbations were observed for $Ru(bpy)_3^{2+}$ in solutions of 1 M tetralkylammonium (methyl or ethyl) chlorides. In the zeolite, both UV−visible and resonance Raman spectroscopy of $Ru(bpy)_3^{2+}$ show no changes on ion-exchanging TEA, indicating minimal perturbation on the ground state. The major spectral perturbations are evident in the emission spectrum and the lifetime. Since no electronic interaction is expected between $Ru(bpy)_3^{2+}$ and TEA, these perturbations in the excited-state properties of $Ru(bpy)_3^{2+}$ in the presence of TEA must arise from other causes. Since TEA carries a unit positive charge, it ion exchanges with one Na^+ in the zeolite. No exchange with Na^+ in sodalite cages is expected. Change in the intrazeolitic water content with the size of the exchanging cation has been discussed by Barrer and co-workers.[28] As expected, the water displaced per cation increased with the volume of the entering cation. The effect was the strongest for organic ions, especially the large alkylammonium ions. Displacement of water from the zeolite to solution is an endothermic process and Barrer and co-workers pointed out that the water molecules that tend to have the weakest interaction with the framework will be displaced initially. Thus, upon ion exchange with TEA, more of the bulklike water from the zeolite will be displaced. Indeed, ion exchange can stop if the water molecules being removed from the zeolites are too strongly held and the costs are too high energetically.

There are roughly 3−4 Na^+ per supercage.[18] Since the radius of TEA (3.37 Å) exceeds the Na^+ (∼1.02 Å) it replaces,[29] it is expected that H_2O molecules that are in the supercages must also be removed with TEA exchange. A maximum of 28 molecules of water can be accommodated in a supercage[30] occupying a volume of 1150 Å^3. Most of these water molecules are bound strongly to the cations and the aluminosilicate framework. The volume of a TEA molecule is 160 Å^3, and so about 6−7 molecules of bulklike water need to be replaced per supercage with the levels of TEA exchange that are being considered here. As the free water molecules are replaced, the medium left behind will resemble more of a "frozen" state, with the remaining H_2O molecules bound to the framework and Na^+ and in a more rigid state.

At this point, it is worthwhile to introduce results of previous studies of $Ru(bpy)_3^{2+}$ that have similarities with what we are observing in zeolites. Four systems appear to be appropriate. First, it has been noted that increases in emission energies and lifetimes are observed in going from a fluid to a rigid medium by lowering the temperature.[31] This is explained by the fact that under frozen conditions, the solvent molecules cannot reorient around the dipolar excited state on the time scale of the excited-state lifetime and therefore do not provide any stabilization of the excited state, and this leads to a blue shift in the emission maximum. The lifetime increase upon freezing is a reflection of the increase in the energy gap. A second system involves $Ru(bpy)_3^{2+}$ in a series of alcohols, in which it was noted that even though E_{00} increased with solvent polarity, the lifetime decreased (increase in k_{nr}), in apparent violation of the energy gap law.[17] This anomaly was explained due to the presence of O−H groups that promoted nonradiative decay, the effect being more pronounced in solvents of higher polarity. A third system involves $Ru(bpy)_3^{2+}$ in sodium lauryl sulfate (NaLS) micellar solutions.[32] It was reported that upon micellization, the emission energy decreased, but the lifetime and quantum yield of emission both increased. It was proposed that the polar headgroups of the micelle rearrange upon excitation of $Ru(bpy)_3^{2+}$ and help stabilize the excited state, but in this process, water molecules get excluded from the vicinity of the micelle-bound $Ru(bpy)_3^{2+}$. The stabilization of the excited state leads to lower emission energies and the lack of H_2O prolonged the excited-state lifetime. The fourth system of interest is a polymerized SiO_2 particle onto whose surface $Ru(bpy)_3^{2+}$ was adsorbed.[33] After several hours of incubation, it was found that the emission spectrum exhibited a marked blue shift with the appearance of two bands at 573 and 606 nm, as compared to 613 nm for the $Ru(bpy)_3^{2+}$ immediately after adsorption. Also, the lifetime and quantum yield of emission increased. It was proposed that the $Ru(bpy)_3^{2+}$ was bound tightly and rigidly just below the SiO_2−water interface. Our observations on the spectral properties of $Ru(bpy)_3^{2+}$ upon changing from Na−Y to TEA−Y most closely correspond with the porous SiO_2 particles.

These four examples provide clues about the observed spectral changes of $Ru(bpy)_3^{2+}$ as Na^+ ions are replaced by TEA. It is now well accepted that the excited state of $Ru(bpy)_3^{2+}$ can best be described as one with a Ru(III) center, with an electron localized on one of the bipyridine ligands.[34] The size of the $Ru(bpy)_3^{2+}$ molecule and the zeolite Y supercage guarantees that once synthesized, the $Ru(bpy)_3^{2+}$ is completely immobilized in the cage. The synthesis of $Ru(bpy)_3^{2+}$ proceeds from the bis complex, $Ru(bpy)_2L_2^{2+}$ to the tris complex. The third bipyridine ligand must approach through a neighboring supercage and once it attaches to the Ru, the complex is immobilized. This implies that in zeolite-entrapped $Ru(bpy)_3^{2+}$, one of the bipyridine ligands must face a neighboring cage through the 7 Å window. Visualization of molecular models of $Ru(bpy)_3^{2+}$ in zeolite Y indicates that for orientations in which one of the bpy ligands face a supercage window, the other two bipyridine ligands must be surrounded by the aluminosilicate framework.[12] This leads to an asymmetric environment around the $Ru(bpy)_3^{2+}$ in the zeolite. Thus, in the excited state of $Ru(bpy)_3^{2+}$, it is highly likely that the electron will be localized on the ligand facing the supercage rather than the ligands facing the negatively charged framework walls, purely for electrostatic reasons. This arrangement also allows for the mobile water molecules in the neighboring cage facing the bipyridine to reorganize and help stabilize the excited state. On the basis of this model, it is then not surprising that the spectral properties of $Ru(bpy)_3^{2+}$ in Na−Y resemble that of a homogeneous aqueous solution. However, upon exchange with TEA, the free, bulklike water molecules that can reorient and provide solvation of the dipolar excited state of $Ru(bpy)_3^{2+*}$ is lost, resulting in the blue-shift of the emission maximum by 30 nm. Increased quantum yields and longer lifetimes are a reflection of the decrease in the nonradiative decay rate constant, as expected from the energy gap law of internal conversion as well as the loss in nonradiative decay pathways via the O−H stretching modes of water.

(d) Implications for the Quenching of the Intrazeolitic $Ru(bpy)_3^{2+}$−Bipyridinium System. For $Ru(bpy)_3^{2+}$−viologen−zeolite Y, exchange of viologen ions into the zeolite will also

result in replacement of the water molecules by virtue of the large size of the organic cation. In parallel with the TEA case, this should lead to increased lifetime, quantum yield, and blue shift of the emission maximum. Such a prediction is borne out by the data obtained with the bipyridinium ions. For $2DQ^{2+}$, with a large driving force for electron-transfer quenching of $Ru(bpy)_3^{2+}$*, the emission is totally quenched at high loading levels. However, for N-$MeDQ^{2+}$, a poorer quencher, it is quite clear that beyond a loading level of 1 bipyridinium molecule per supercage, quenching actually decreases. The reason is that at higher loadings, water content is diminishing, resulting in an increase of emission intensity of $Ru(bpy)_3^{2+}$*. This leads to higher residual emission after quenching since the initial quantum yield of the emission has increased. The correctness of this explanation is also evident from the fact that there is a blue-shift of the residual emission for N-$MeDQ^{2+}$, consistent with the direction of spectral shifts observed in the presence of TEA. However, the magnitudes of these shifts are quite different. In the case of N-$MeDQ^{2+}$, the emission maximum is at 591 nm, whereas for TEA it is at 605 nm. This could be a reflection of the difference in the volumes of the ions and their loading levels. The volume of the N-$MeDQ^{2+}$ molecule was calculated to be 314 $Å^3$, and therefore at the highest loadings of 1.4 molecules per supercage, the number of H_2O molecules displaced is about 14−15, almost twice as much as replaced with TEA.

Two aspects of $Ru(bpy)_3^{2+}$ entrapment in zeolite Y are relevant for photoelectron transfer to acceptor molecules in neighboring cages. First is the fact that the electron in the photoexcited $Ru^{III}(bpy)_2(bpy)^{\bullet-}$ resides on the ligand facing the acceptor molecule through the 7 Å window. Second, the interest in use of polypyridyl complexes of Ru(II) as sensitizers arises from the long lifetime of the excited ^{3}MLCT state.[20] Encapsulation into the zeolite and subsequently being surrounded by large electron acceptor molecules should lengthen the lifetime of $Ru(bpy)_3^{2+}$* even further and promote the extent of the forward electron-transfer reaction. These features, to the best of our knowledge are unique to the intrazeolitic space and arises because the volume inside the zeolite is fixed and with the packing of quencher molecules, the "solvent" environment undergoes a dramatic change.

Conclusions

The excited-state properties of $Ru(bpy)_3^{2+}$ encapsulated in Na−Y resemble that in water. However, upon exchange of the Na^+ ions by TEA, the emission spectrum exhibits a blue shift of 21 to 605 nm. The emission yield increases by a factor of 2.7 and the lifetime of the excited state of $Ru(bpy)_3^{2+}$ increases by a factor of 2 to 1220 ns. Temperature-dependent lifetime studies indicate that the nonradiative decays occur from the 3-fold MLCT states as well as a fourth MLCT state ~800 cm^{-1} higher in energy. The large TEA ions replace the bulklike free water molecules in the supercages. In the absence of the water molecules, stabilization of the dipolar excited-state $Ru^{III}(bpy)_2(bpy)^{\bullet-}$ is reduced and results in a blue shift of the emission maxima. Increases in lifetime and quantum yield occur due to the increase in the energy gap as well as the absence of the water molecules, which promote nonradiative decay. Bipyridinium ions that quench the excited state of $Ru(bpy)_3^{2+}$ oxidatively will also replace the water molecules in the supercages and have the same influence as TEA. This was evident from spectroscopic studies with an inefficient quencher molecule, N-$MeDQ^{2+}$. It was found that at intrazeolitic loading levels exceeding 1 molecule of N-$MeDQ^{2+}$ per supercage, the quenching of the excited $Ru(bpy)_3^{2+}$ actually decreased. The reason for this anomaly is that at higher loading levels of N-$MeDQ^{2+}$, enough water molecules are being replaced from the supercages, leading to increase in emission yields of excited $Ru(bpy)_3^{2+}$.

Acknowledgment. We thank DOE, Basic Sciences Division for funding this study.

References and Notes

(1) Dutta, P. K.; Ledney, M. *Prog. Inorg. Chem.* **1997**, *44*, 209.

(2) *Photochemistry in Organized and Constrained Media*; Ramamurthy, V., Ed.; VCH: New York, 1991.

(3) DeWIlde, W.; Peeters, G.; Lunsford, J. H. *J. Phys. Chem.* **1980**, *84*, 2306.

(4) Incavo, J. A.; Dutta, P. K. *J. Phys. Chem.* **1990**, *94*, 3075.

(5) Maruszeweski, K.; Strommen, D. P.; Kincaid, J. R. *J. Am. Chem. Soc.* **1993**, *115*, 8345.

(6) Sykora, M.; Kincaid, J. R.; Dutta, P. K.; Castagnola, N. B. *J. Phys. Chem. B* **1999**, *103*, 309.

(7) Rillema, D. P.; Jones, D. S.; Levey, H. A. *J. Chem Soc., Chem. Commun.* **1979**, 849.

(8) Kruger, J. S.; Mayer, J. E.; Mallouk, T. E. *J. Am. Chem. Soc.* **1988**, *110*, 8232.

(9) Borja, M.; Dutta, P. K. *Nature* **1993**, *362*, 43.

(10) Yonemoto, E. H.; Kim, Y. I.; Shcmehl, R. H.; Wallin, J. O.; Shoulder, B. A.; Richardson, B. R.; Haw, J. F.; Mallouk, T. E. *J. Am. Chem. Soc.* **1994**, *116*, 10557.

(11) Sykora, M.; Kincaid, J. R. *Nature* **1997**, *387*, 162.

(12) Vitale, M.; Castagnola, N. B.; Ortins, N. J.; Brooke, J. A.; Vaidyalingam, A.; Dutta, P. K. *J. Phys. Chem. B* **1999**, *103*, 2408.

(13) Allsopp, S. R.; Cox, A.; Kemp, T. J.; Reed, W. J. *J. Chem. Soc., Faraday Trans. 1* **1978**, *79*, 1275.

(14) Gaines, G. L. *Inorg. Chem.* **1980**, *19*, 1710.

(15) Caspar, J. V.; Meyer, T. J. *J. Am. Chem. Soc.* **1983**, *105*, 5583.

(16) Sykora, M.; Kincaid, J. R. *Inorg. Chem.* **1995**, *34*, 5852.

(17) Hartmann, P.; Leiner, M. J.; Draxler, S.; Lippitsch, M. E. *Chem. Phys.* **1996**, *207*, 137.

(18) Breck, D. W. *Zeolite Molecular Sieves*; Krieger: Malibar, FL, 1974.

(19) Albery, W. J.; Bartlett, P. N.; Wilde, C. P.; Darwent, J. R. *J. Am. Chem. Soc.* **1985**, *107*, 1854.

(20) (a)Meyer, T. J. *Pure Appl. Chem* **1986**, *58*, 1193. (b) Durham, B.; Caspar, J. V.; Nagle, J. K.; Meyer, T. J. *J. Am. Chem. Soc.* **1982**, *104*, 4803.

(21) Amouyal, E.; Zidler, B. *Isr. J. Chem.* **1982**, *22*, 117.

(22) Kober, E. M.; Caspar, J. V.; Lumpkin, R. S.; Meyer, T. J. *J. Phys. Chem.* **1986**, *90*, 3722.

(23) Barqawi, K. R.; Murtaza, Z.; Meyer, T. J. *J. Phys. Chem.* **1991**, *95*, 47.

(24) Bolletta, F.; Juris, A.; Maestri, M.; Sandrini, D. *Inorg. Chim. Acta* **1980**, *44*, L175.

(25) (a) Yersin, H.; Gallhuber, E.; Voglet, A.; Kunkely, H. *J. Am. Chem. Soc.* **1983**, *105*, 4155. (b) Yersin, H.; Gallhuber, E. *J. Am. Chem. Soc.* **1984**, *106*, 6582. (c) Yersin, H.; Gallhuber, E.; Hensler, G. *Chem. Phys. Lett.* **1987**, *134*, 497.

(26) Lumpkin, R. S.; Kober, E. M.; Worl, L. A.; Murtaza, Z.; Meyer, T. J. *J. Phys. Chem.* **1990**, *94*, 239.

(27) Allen, G. H.; White, R. P.; Rillema, D. P.; Meyer, T. J. *J. Am. Chem. Soc.* **1984**, *106*, 2613.

(28) (a) Barrer, R. M.; Papadopoulos, R.; Rees, L. V. C. *J. Inorg. Nucl. Chem.* **1969**, *29*, 2047. (b) Barrer, R. M.; Meier, W. M. *Trans. Faraday Soc.* **1958**, *54*, 1074.

(29) Marcus, Y.; Hefter, G.; Pang, T.-S. *J. Chem. Soc., Faraday Trans 1* **1994**, *90*, 1899.

(30) Ramamurthy, V. *Photochemistry in Organized and Constrained Media*; Ramamurthy, V., Ed.; VCH: New York, p 429.

(31) (a) Barigelletti, F.; Belser, P.; von Zelewsky, A.; Juris, A.; Balzani, V. *J. Phys. Chem.* **1985**, *89*, 3680. (b) Lumpkin, R. S.; Meyer, T. J. *J. Phys. Chem.* **1986**, *90*, 5307.

(32) Dressick, W. J.; Cline, J., III; Demas, J. N.; DeGraff, B. A. *J. Am. Chem. Soc.* **1986**, *108*, 7567.

(33) Wheeler, J.; Thomas, J. K. *J. Phys. Chem.* **1982**, *86*, 4541.

(34) Ferguson, J.; Krausz, E. R.; Maeder, M. *J. Phys. Chem.* **1985**, *89*, 1852.